DEPTH-VARIANT IMAGE RESTORATION IN 3D FLUORESCENCE MICROSCOPY: TWO APPROACHES UNDER GAUSSIAN AND POISSONIAN NOISE CONDITIONS

S. Ben Hadj, L. Blanc-Féraud*

Morphème Research Group,
I3S/CNRS/INRIA/UNSA/IBDC,
2000, route des Lucioles,
06903 Sophia Antipolis Cedex, France

E. Maalouf, B. Colicchio, A. Dieterlen*

MIPS Laboratory,
UHA/IUT of Mulhouse,
61, rue Albert Camus, 68093 Mulhouse, France

ABSTRACT

In this article, we are interested in restoring images from 3D fluorescence microscopy. In fact, these images are affected by a depth-variant blur due to light refraction phenomenon. We present and compare two different restoration strategies for that problem. The first one is based on multiple deconvolutions with depth-invariant blur functions and the second one consists in using a depth-variant blur function in the deconvolution process. Furthermore, we fit two deconvolution algorithms to this problem. First, we use the Richardson-Lucy method with total variation regularization to restore confocal microscopy images which are affected by a Poisson noise. Then, we focus on restoring wide field microscopy images which are corrupted by a Gaussian noise. Tests on simulated data show that the second restoration strategy is slightly more accurate than the first one for both noise conditions.

Index Terms— Depth-variant blur, energy minimization, fluorescence microscopy, noise, PSF, restoration.

1. INTRODUCTION

Fluorescence microscopy is a powerful imaging technique that provides 3D images of biological living specimen. However, facing some inherent optical limits (e.g. light diffraction), it is essential to remove the blur and noise present in these images by digital processing in order to provide biologist with suitable images for quantitative studies. Many restoration methods in the context of space-invariant (SI) blur were developed ([1] and references therein). In these methods, the image degradation model is a convolution between the original image and the system induced blur function called Point Spread Function (PSF). However, due to the refractive index mismatch between the different mediums composing the system and the biological sample, the 3D blur function is varying along the z-axis i.e. the depth of the source point in the specimen. Considering a pointwise varying PSF is computationally prohibitive, especially when dealing with 3D images. To avoid the intensive computing time, many existing restoration methods consider a piecewise-invariant PSF [2]. However, this usually leads to blocking effect in the restored image. To overcome this problem, an interpolation technique of adjacent PSF is proposed in [3]. In this article, we present and discuss two restoration strategies for images degraded with a depth-variant (DV) blur. The first one is based on multiple deconvolutions with a SI PSF and the second one consists in using a DV blur function in the deconvolution process. We test and compare these two approaches on simulated images of fluorescence microscopy. In particular, we compare their ease of implementation, computing time and accuracy. For that, we rely on two deconvolution procedures which are developed for SI PSF. On the one hand, we use the Richardson-Lucy method with Total Variation regularization (RLTV) [1] which is carried out under Poisson noise assumption in order to restore Confocal Laser Scanning Microscopy (CLSM) images. On the other hand, we use an other method with total variation regularization adapted to images with an additive Gaussian noise in order to restore Wide Field Microscopy (WFM) images. For that, we rely on a fast optimization method based on a domain-decomposition technique [4]. This article is organized as follows: in the second section, we present the two DV restoration techniques. In the third section, we develop and compare both techniques based on the RLTV method. In the fourth section, we also compare these methods using the deconvolution method proposed in [4]. To conclude, some perspectives are proposed.

2. TWO DV RESTORATION APPROACHES

2.1. Enhanced Merging Masks Algorithm (EMMA)

In the method proposed in [5], a set of 3D PSF $\{h_1, ..., h_N\}$ is supposed to be given at different depths either theoretically by using for instance the mathematical model of Gibson and Lanni [6] or experimentally by imaging some sub-resolution

* Thanks to ANR DIAMOND for funding and P. Pankajakshan for clarifying many aspects about CLSM and providing the theoretical PSF generation software.

beads that can be assimilated to punctual light sources. The steps of this algorithm are summarized in Fig. 1(left). After

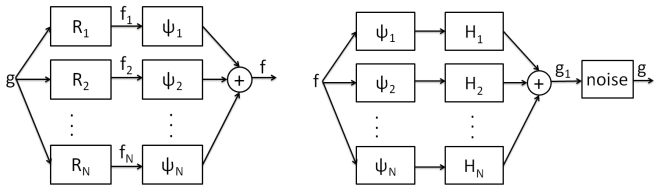


Fig. 1. left: DV restoration using EMMA. R_i, $i = 1, ..., N$ refers to the restoration with the SI convolution kernel h_i, right: DV blur modeling considering $\widetilde{H}$.

defining this PSF set, multiple deconvolution of the degraded image g can be done separately, each with a different PSF h_i, using any classical deconvolution algorithm depending on the data to restore, yielding to a set of deconvolved images $\{f_1, ..., f_N\}$. These resulting images are then merged together using adequate masks $\{\psi_1, ..., \psi_N\}$ that select the best part of each result f_i while smoothing transitions between these parts to form the final estimate f i.e. the resulting image is given by: $f(u) = \sum_{i=1}^{N} \psi_i(z) . f_i(u)$, where $u = (x, y, z)$ is a voxel in the 3D domain Ω. In fact, the region presenting the minimal error in each restoration f_i is around the used PSF position. That's why, we propose to use convenient triangular mask functions only varying along the z-axis as the blur is supposed to be shift-invariant along x and y axis. Each mask ψ_i associated with the PSF h_i equals 1 at the PSF position and decreases linearly when going away from this position to reach zero when achieving adjacent PSF positions (cf Fig. 2).

2.2. Restoration with a DV PSF

Although the previous strategy is simple to implement and can be applied for any restoration algorithm designed for a SI PSF, an other way to deal with DV blurred image is using a DV PSF in the deconvolution process. In every iteration of the deconvolution algorithm, each point of the image is actually deconvolved by its corresponding approximate PSF. For that purpose, we use an efficient DV blur model previously proposed in [7]. This model is illustrated in Fig. 1(right). In essence, the blurred image g_1 is obtained by applying a DV operator $\widetilde{H}$ to the true image f: $g_1 = \widetilde{H}(f)$ where $\widetilde{H}(f) = \sum_{1 \leq i \leq D} H_i(\psi_i . f)$ and $H_i(.) = h_i * .$ is the convolution with the SI PSF h_i. In this case, classical deconvolution methods [1] must be adapted to such a DV operator.

3. RESTORATION IN A FRAMEWORK OF POISSON NOISE

In this section, we look for restoring images from CLSM system which are degraded with a DV blur and corrupted with a Poisson noise due to the low illumination light. A commonly used image restoration method in such a situation is the Richardson-Lucy algorithm with total variation regularization (RLTV). We explore this algorithm to simultaneously remove the DV blur and the noise using the two techniques presented in the previous section.

3.1. RLTV method for DV restoration

The RLTV method is an iterative algorithm which maximizes the posterior probability using a multiplicative gradient-descent scheme. It consists in iterating this equation: $f^{k+1} = \frac{f^k}{1 - \alpha div\left(\frac{\nabla f^k}{|\nabla f^k|}\right)} . H^*\left(\frac{g}{H(f^k)}\right)$ where $k+1$ is the current iteration, ∇ is the gradient operator, $div(.)$ is the divergence operator and $\alpha > 0$ is a fixed regularization parameter. The EMMA restoration given in Fig. 1(left) consists in repeating this algorithm on the entire image for different PSF, then merging the results. However, for the second proposed method given in Fig. 1(right), a study of the RLTV method for the DV blur operator $\widetilde{H}$ is needed. Indeed, an estimate of the original image is accessible by minimizing the following cost function: $J_1(f) = \left[\sum_u \widetilde{H}(f)(u) - g(u) log\left(\widetilde{H}(f)(u)\right)\right] + \alpha \|\nabla f\|_1$. As the criterion is convex, a minimum of J_1 is tractable by canceling its partial derivative w.r.t f, which is expressed as: $\frac{\partial J_1}{\partial f}(f) = \widetilde{H}^*(1) - \widetilde{H}^*\left(\frac{g}{\widetilde{H}(f)}\right) - \alpha\, div\left(\frac{\nabla f}{|\nabla f|}\right)$ where $\widetilde{H}^*$, the adjoint of $\widetilde{H}$, is written in this way: $\widetilde{H}^*(.) = \sum_{i=1}^{N} \psi_i . H_i^*(.)$ with H_i^* the adjoint of H_i. As $\sum_{i=1}^{N} \psi_i(z) = 1$, $\forall z$, we can show that $\widetilde{H}^*(1) = 1$ and thus obtain a similar iteration as that for a SI filter.

3.2. Test and comparison

Our first test was conducted over a simulated image of a CLSM system having a magnification of $100X$, a numerical aperture of 1.2 and an oil immersed objective with a refractive index of 1.515. The beads are supposed to be immersed in water of refractive index of 1.33. Wavelengths of excitation and emission lights are respectively equal to $560\,nm$ and $600\,nm$. The system is assumed to have a pinhole diameter of $650\,AU$. Furthermore, lateral and axial sampling are respectively set to $0.06\,\mu m$ and $0.25\,\mu m$ respecting Nyquist sampling. Knowing all these parameters, the PSF are computed using the mathematical model presented in [6]. We consider a synthesized object of four spherical beads having each a diameter of $2.25\,\mu m$ (cf. Fig. 3(a)). The simulated observation of $128 \times 128 \times 128$ voxels (cf.Fig. 3(b)) is obtained by blurring the original image using 128 PSF, each computed at a different depth and then adding to it a Poisson noise. Multiple 2D convolutions are computed in the Fourier domain since the blur is SI along X and Y. The basic difference

between these used PSFs of a CLSM system is a shift of the PSF from its central plane depending on the considered depth, leading to a shift of the blurred beads from their original positions. DV restoration is done using 20 PSF selected in such a way that the correlation coefficient between two successive PSF is not less than 0.9, starting from the PSF at zero depth. Associated mask functions are displayed in Fig. 2. (X, Z)

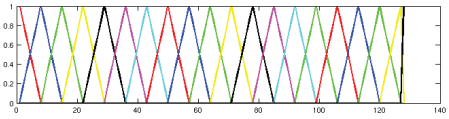
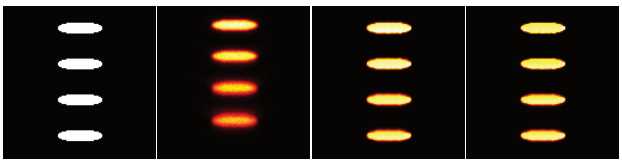


Fig. 2. A set of 20 weighting functions varying with Z.

slices of the restored images using the two proposed methods (see Fig. 3(c) and (d)) as well as intensity profiles passing through bead centers (cf. Fig. 4) along the z-axis show the relevance of both methods. In order to assess their accuracy and rapidity, we present in table 1, the mean for 30 noise realizations of the relative standard error (RSE), the structural similarity index (SSIM) between each of the restored images and the original one as well as the mean computing time for each method. Tests were performed on a machine having 8 cores of frequency $2.40\,GHz$. According to these values, we remark that restoration with $\widetilde{H}$ is slightly more accurate and largely faster than EMMA Nevertheless, note that EMMA can be easily parallelized and thus the computing time can be significantly reduced.



(a) (b) (c) (d)

Fig. 3. Restoration under Poisson noise condition: (X,Z) slices of (a) the object, (b) the observation, (c) the restoration using EMMA, (d) the restoration using $\widetilde{H}$.

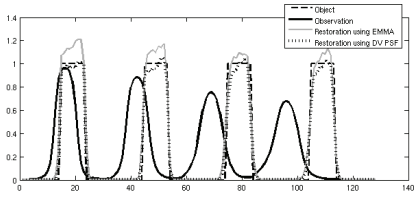


Fig. 4. Intensity profiles along the z-axis of the object (dash), the observation (bold-continuous), the restoration using EMMA (gray-continuous), and the restoration using $\widetilde{H}$ (dot). Restorations are based on the RLTV algorithm.

4. RESTORATION IN A FRAMEWORK OF GAUSSIAN NOISE

In this section, we deal with images that are degraded with a DV blur and an additive Gaussian noise such as those coming from WFM. As we did in the previous section, we minimize an energy criterion with a total variation regularization. For that, we rely on a recent optimization technique [4] where the complexity of the problem is reduced by decomposing it in smaller sub-problems and treating them in a parallel way. We apply this method using the two strategies presented in subsections 2.1 and 2.2.

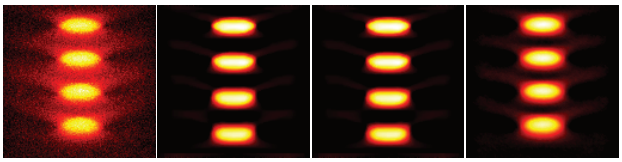
4.1. Fornasier et al method for DV restoration

Considering a SI PSF, the estimate of the original image f is accessible by minimizing the following cost function which is formed by two terms: a quadratic term corresponding to data fidelity in presence of Gaussian noise and a total variation regularization term: $J_2(f) = \|H(f) - g\|_2^2 + \alpha \|\nabla f\|_1$. The idea of Fornasier et al. [4] consists in splitting the image domain Ω into overlapping sub-domains, say for example a splitting into two sub-domains Ω_1 and Ω_2 for sake of clarity. Consequently, the solution of the problem is also decomposed as follows: $f(u) = \begin{cases} f_1(u) & if\ u \in \Omega_1 \setminus \Omega_2 \\ f_1(u) + f_2(u) & if\ u \in \Omega_1 \cap \Omega_2 \\ f_2(u) & if\ u \in \Omega_2 \setminus \Omega_1 \end{cases}$. Minimization in each sub-domain to estimate f_1 and f_2 is performed under certain constraints on the boundaries between neighboring sub-domains. For that problem, Fornasier et al propose to use a *Lagrange multiplier* scheme. It consists in minimizing an auxiliary function of $J_2(.)$ where variables f_1 and f_2 are not affected by the action of H so that the solution is directly accessible via an *oblique thresholding* theorem. The interested reader should refer to [4] for further details about this algorithm. Now, to restore DV blurred image using EMMA, it suffices to apply this procedure for a collection of SI PSF and then combining the results. DV restoration using the second proposed technique (sub-section 2.2) is tractable by replacing in this procedure the SI operator H by the DV one $\widetilde{H}$ and the adjoint of H by $\widetilde{H}^*$. Several conditions should be verified in order to ensure existence, uniqueness and convergence of the proposed solution. Among them we verify that $\left\|\widetilde{H}\right\|_2 < 1$ in [8].

4.2. Test and comparison

The blurring system is now a WFM having the same characteristic as the previously considered system. We also use the same bead image of Fig. 3(a). After blurring it with 128 PSFs, each corresponds to a given depth, we add to it a Gaussian noise. The obtained distorted image having a signal to noise ratio of about $30\,dB$ is presented in Fig. 5(a). Restoration results using 10 PSF combined with EMMA and the sec-

ond method using $\widetilde{H}$ are respectively depicted in Fig. 5(b) and (c). In order to show the interest of the DV restoration approaches, we depict in Fig. 5(d) the restoration result with a SI PSF computed at a zero depth. Corresponding intensity profiles are displayed in Fig. 6. Better results can be achieved by using more PSFs [9]. Table 1 shows that both restoration methods have practically the same precision. Indeed, the error of the approximate DV blur modeling was dominated by the error introduced by the inversion method due to the ill-posed problem. Note that using Fornasier et al method and a small intersection between 2 sub-domains, we gain about 30% of the computing time spent by ADM method [10].



(a) (b) (c) (d)

Fig. 5. Restoration under Gaussian noise condition: (X,Z) slices of (a) the observation, (b) the restoration using EMMA, (c) the restoration using $\widetilde{H}$, and (d) restoration with a SI PSF.

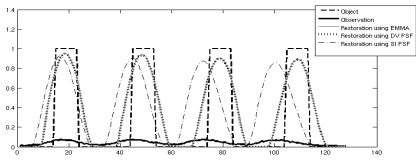


Fig. 6. Intensity profiles along the z-axis associated with restoration under Gaussian noise. Same plot lines as those of Fig. 4 are used, restoration with a SI PSF plotted in dash-dot.

	EMMA method		Restoration with $\widetilde{H}$	
Noise	Poisson	Gauss	Poisson	Gauss
RSE mean (%)	6.12	32.22	5.25	32.02
SSIM mean	0.96	0.743	0.97	0.746
Mean time (mn)	28	25	12	8

Table 1. Comparing DV restoration methods (Fig. 1).

5. CONCLUSION

In this article, we presented two methods to restore fluorescence microscopy images taking into account the blur variation along the z-axis. In the first method, the image is restored with different SI PSF. The results are then merged together using adequate mask functions. In the second method, a DV blur function is used in the deconvolution process. Tests on simulated images of CLSM and WFM showed that the second method is slightly more accurate than the first one. An other interesting result is the computing time which is smaller for the second method. More tests on different images with other noise realizations as well as tests on real data are under considerations and will be presented at the conference. Finally, our future interest will be extending the proposed methods to the blind restoration case.

6. REFERENCES

[1] N. Dey, L. Blanc-Féraud, C. Zimmer, Z. Kam, P. Roux, J.C. Olivo-Marin, and J. Zerubia, "Richardson-lucy algorithm with total variation regularization for 3d confocal microscope deconvolution," *Microscopy Research Technique*, vol. 69, pp. 260–266, 2006.

[2] C. Preza and J.A. Conchello, "Image estimation accounting for point spread function depth variation in three-dimensional fluorescence microscopy," in *SPIE*, 2003, vol. 4964, p. 1336.

[3] C. Preza and J.A. Conchello, "Depth-variant maximum-likelihood restoration for three-dimensional fluorescence microscopy," *JOSA A*, vol. 21, no. 9, pp. 1593–1601, 2004.

[4] M. Fornasier, A. Langer, and C.B. Schnlieb, "A convergent overlapping domain decomposition method for total variation minimization," *Numerische Mathematik*, pp. 1–41, 2009.

[5] E. Maalouf, "Contribution to fluorescence microscopy, 3d thick samples deconvolution and depth-variant PSF," in *Ph.D. thesis, UHA*, Mulhouse, France, 2010.

[6] S. F. Gibson and F. Lanni, *Measured and analytical point spread functions of the optical microscope for use in 3-D optical serial sectioning microscopy*, Optical Microscopy for Biology, Wiley-Liss, New York, 1990.

[7] M. Hirsch, S. Sra, B. Scholkopf, and S. Harmeling, "Efficient filter flow for space-variant multiframe blind deconvolution," in *IEEE CVPR*, 2010, pp. 607–614.

[8] S. Ben Hadj and L. Blanc-Féraud, "Restoration method for spatially variant blurred images," in *INRIA research report*, 2011, number 7654.

[9] C. Preza and V. Myneni, "Quantitative depth-variant imaging for fluorescence microscopy using the cosmos software package," *Three-Dimensional and Multidimensional Microscopy: Image Acquisition and Processing XVII, BiOS, SPIE*, pp. 7570–2, 2010.

[10] M. Ng, P. Weiss, and X.M. Yuan, "Solving constrained total-variation image restoration and reconstruction problems via alternating direction methods," *SIAM journal on Scientific Computing*, vol. 32, pp. 2710–2736, 2010.